

## TOWARDS A DETERMINATION OF THE SPECTRUM OF QCD USING A SPACE-TIME LATTICE

K.J. JUGE, A. LICHTL AND C. MORNINGSTAR\*

*Department of Physics, Carnegie Mellon University, Pittsburgh, PA 15213, USA*

R.G. EDWARDS AND D.G. RICHARDS

*Thomas Jefferson National Accelerator Facility, Newport News, VA 23606, USA*

S. BASAK AND S. WALLACE

*Department of Physics, University of Maryland, College Park, MD 20742, USA*

I. SATO

*Lawrence Berkeley Laboratory, 1 Cyclotron Road, Berkeley, CA 94720, USA*

G.T. FLEMING

*Sloane Physics Laboratory, Yale University, New Haven, CT 06520, USA*

Progress by the Lattice Hadron Physics Collaboration in determining the baryon and meson resonance spectrum of QCD using Monte Carlo methods with space-time lattices is described. The extraction of excited-state energies necessitates the evaluation of correlation matrices of sets of operators, and the importance of extended three-quark operators to capture both the radial and orbital structures of baryons is emphasized. The use of both quark-field smearing and link-field smearing in the operators is essential for reducing the couplings of the operators to the high-frequency modes and for reducing statistical noise in the correlators. The extraction of nine energy levels in a given symmetry channel is demonstrated, and identifying the continuum spin quantum numbers of the levels is discussed.

### 1. Introduction

A charge from the late Nathan Isgur to use Monte Carlo methods to extract the spectrum of hadron resonances and hadronic properties resulted in the formation of the Lattice Hadron Physics Collaboration (LHPC) in the

---

\*Speaker.

year 2000. As part of a national collaboration of lattice QCD theorists, the LHPC acquired funding from several sources, including the DOE's Scientific Discovery through Advanced Computing initiative, to build large computing clusters at JLab, Fermilab, and Brookhaven, as well as to develop the software to carry out the needed large-scale computations. The LHPC has several broad goals: to compute the spectrum of QCD from first principles, to investigate hadron structure by computing form factors, structure functions, and other matrix elements, and to study hadron-hadron interactions. This talk focuses solely on our efforts to determine the spectrum of QCD.

Extracting the spectrum of resonances in QCD is a big challenge. The determination of excited-state energies requires the use of correlation matrices of sets of operators. The masses and widths of unstable hadrons (resonances) must be deduced from the energies of single-particle and multi-hadron stationary states in a finite-sized box. This necessitates the use of multi-hadron operators in the correlation matrices, and the computations must be performed in full QCD at realistically-light quark masses. For these reasons, the computation of the QCD spectrum is indeed a long-term project. This talk is a brief status report of our efforts.

I first describe in Sec. 2 how excited-state energies are extracted in our Monte Carlo calculations, and discuss issues related to unstable resonances. Our construction of baryon operators is then outlined in Sec. 3 (see Ref. 1 for further details), and in Sec. 4, the importance of using smeared quark and gluon fields is demonstrated. (see also Ref. 2). The first-time extraction of *nine* nucleon energy levels is also presented in this section. Concluding remarks are made and future work is outlined in the concluding Sec. 5.

## 2. Excited states and resonances

In the path integral formulation of quantum field theory with imaginary time, stationary-state energies are extracted from the asymptotic decay rates of temporal correlations of the field operators. If  $\Phi(t)$  is a Heisenberg-picture operator which annihilates the hadron of interest at time  $t$ , then its evolution  $\Phi(t) = e^{Ht}\Phi(0)e^{-Ht}$ , where  $H$  is the Hamiltonian, can be used to show that in a finite-sized box,

$$C(t) \equiv \langle 0 | \Phi(t) \Phi^\dagger(0) | 0 \rangle = \sum_n \langle 0 | e^{Ht} \Phi(0) e^{-Ht} | n \rangle \langle n | \Phi^\dagger(0) | 0 \rangle, \quad (1)$$

$$= \sum_n |\langle 0 | \Phi(0) | n \rangle|^2 e^{-(E_n - E_0)t} = \sum_n A_n e^{-(E_n - E_0)t}, \quad (2)$$

where  $\{|n\rangle\}$  is the complete set of discrete eigenvectors of  $H$ . We assume the existence of a transfer matrix, and temporal boundary conditions have been ignored for illustrative purposes. One can then extract  $A_1$  and  $E_1 - E_0$  as  $t \rightarrow \infty$ , assuming  $\langle 0|\Phi(0)|0\rangle = 0$  and  $\langle 0|\Phi(0)|1\rangle \neq 0$ .

A convenient visual tool for demonstrating energy-level extraction is the so-called ‘‘effective mass’’ defined by  $m_{\text{eff}}(t) = \ln[C(t)/C(t+a_t)]$ , where  $t$  is time and  $a_t$  is the temporal lattice spacing. The effective mass tends to the actual mass (or energy) of the ground state as  $t$  becomes large, signalled by a plateau in the effective mass. At smaller times before this plateau is observed, the effective mass varies due to contributions from other states in the spectrum. The correlation  $C(t)$  is estimated with some statistical uncertainty since the Monte Carlo method is used, and usually, the ratio of the noise to the signal increases with temporal separation  $t$ . Hence, judiciously-chosen operators having reduced couplings with contaminating higher-lying states are important in order to observe a plateau in the effective mass before noise swamps the signal. Key ingredients in constructing such operators are the use of smeared quark and gluon fields, the incorporation of spatially-extended assemblages of the fields, and the use of sets of different operators to exploit improvements from variational methods.

Methods of extracting excited-state energies are well known<sup>3,4</sup>. For a given  $N \times N$  Hermitian matrix of correlations  $C_{\alpha\beta}(t) = \langle 0|\Phi_\alpha(t)\Phi_\beta^\dagger(0)|0\rangle$ , the  $N$  *principal correlators*  $\lambda_\alpha(t, t_0)$  are defined as the eigenvalues of the matrix  $C(t_0)^{-1/2}C(t)C(t_0)^{-1/2}$ , where  $t_0$  is some reference time (typically small), and one can show that

$$\lim_{t \rightarrow \infty} \lambda_\alpha(t, t_0) = e^{-(t-t_0)E_\alpha} (1 + O(e^{-t\Delta E_\alpha})), \quad \Delta E_\alpha = \min_{\beta \neq \alpha} |E_\beta - E_\alpha|, \quad (3)$$

assuming  $E_0 = 0$  and  $\lambda_1 \geq \lambda_2 \geq \lambda_3 \dots$ . The  $N$  principal effective masses  $m_\alpha^{\text{eff}}(t) = \ln[\lambda_\alpha(t, t_0)/\lambda_\alpha(t+a_t, t_0)]$  now tend (plateau) to the  $N$  lowest-lying stationary-state energies which couple to the  $N$  operators. The associated eigenvectors are orthogonal, and a knowledge of the eigenvectors can yield information about the partonic structure of the states.

Many of the hadron states we wish to study are unstable resonances. Our computations are done out of necessity in a box of finite volume with periodic boundary conditions. Hence, the momenta of the particles we study are quantized, so all states are discrete in our computations. Thus, we can only determine the discrete energy spectrum of stationary states in a periodic box, which are admixtures of single hadrons and multi-hadron states. Resonance masses and widths must somehow be deduced from the finite-box spectrum<sup>5,6,7,8</sup>. Once the masses of the stable single particle

Table 1. Continuum limit spin identification: the number  $n_{\Lambda}^J$  of times that the  $\Lambda$  irrep. of the octahedral point group  $O_h$  occurs in the (reducible) subduction of the  $J$  irrep. of  $SU(2)$ . The numbers for  $G_{1u}, G_{2u}, H_u$  are the same as for  $G_{1g}, G_{2g}, H_g$ , respectively.

$J$	$n_{G_{1g}}^J$	$n_{G_{2g}}^J$	$n_{H_g}^J$	$J$	$n_{G_{1g}}^J$	$n_{G_{2g}}^J$	$n_{H_g}^J$
$\frac{1}{2}$	1	0	0	$\frac{9}{2}$	1	0	2
$\frac{3}{2}$	0	0	1	$\frac{11}{2}$	1	1	2
$\frac{5}{2}$	0	1	1	$\frac{13}{2}$	1	2	2
$\frac{7}{2}$	1	1	1	$\frac{15}{2}$	1	1	3

states have been determined, the placement and pattern of their scattering states are known approximately, and the dependences of their energies on the volume are roughly known. Resonances show up as extra states with little volume dependence. Our initial goal is simply to ferret out these resonances, not to pin down their properties to high precision.

### 3. Operator construction

Our approach to constructing hadron operators is to directly combine the physical characteristics of hadrons with the symmetries of the lattice regularization of QCD used in simulations. For baryons at rest, our operators are formed using group-theoretical projections onto the irreducible representations (irreps) of the  $O_h$  symmetry group of a three-dimensional cubic lattice. There are four two-dimensional irreps  $G_{1g}, G_{1u}, G_{2g}, G_{2u}$  and two four-dimensional representations  $H_g$  and  $H_u$ . The continuum-limit spins  $J$  of our states must be deduced by examining degeneracy patterns across the different  $O_h$  irreps (see Table 1). For example, a  $J^P = \frac{1}{2}^+$  state will show up in the  $G_{1g}$  channel without degenerate partners in the other channels, and a  $J^P = \frac{3}{2}^+$  state will show up in the  $H_g$  channel without degenerate partners in the other channels. Four of the six polarizations of a  $J^P = \frac{5}{2}^+$  state show up as a level in the  $H_g$  channel, and the other two will occur as a degenerate partner in the  $G_{2g}$  channel, whereas three degenerate levels, one in each of the three  $G_{1g}, G_{2g}, H_g$  channels, may indicate a single  $J^P = \frac{7}{2}^+$  state (or the accidental degeneracy of a spin- $\frac{1}{2}$  and a  $\frac{5}{2}$  state).

Baryons are expected to be rather large objects, so local operators will not suffice. Our approach to constructing spatially-extended operators is to use covariant displacements of the quark fields along the links of the lattice. Displacements in different directions are used to build up the appropriate

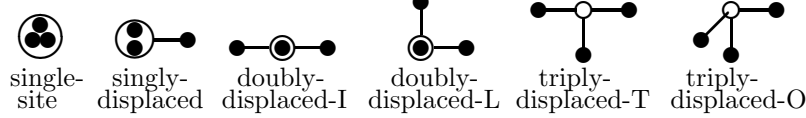


Figure 1. The spatial arrangements of the extended three-quark baryon operators used. Smeared quark fields are shown by solid circles, line segments indicate gauge-covariant displacements, and each hollow circle indicates the location of a Levi-Civita color coupling. For simplicity, all displacements have the same length in an operator.

orbital structure, and displacements of different lengths can build up the needed radial structure. All our three-quark baryon operators are superpositions of gauge-invariant, translationally-invariant terms of the form

$$\Phi_{\alpha\beta\gamma,ijk}^{ABC}(t) = \sum_{\vec{x}} \varepsilon_{abc} (\tilde{D}_i^{(p)}\tilde{\psi}(\vec{x}, t))_{a\alpha}^A (\tilde{D}_j^{(p)}\tilde{\psi}(\vec{x}, t))_{b\beta}^B (\tilde{D}_k^{(p)}\tilde{\psi}(\vec{x}, t))_{c\gamma}^C, \quad (4)$$

where  $A, B, C$  indicate quark flavor,  $a, b, c$  are color indices,  $\alpha, \beta, \gamma$  are Dirac spin indices,  $\tilde{\psi}$  indicates a smeared quark field, and  $\tilde{D}_j^{(p)}$  denotes the smeared  $p$ -link covariant displacement operator in the  $j$ -th direction. The smearing of the quark and gauge field will be discussed later. There are six different spatial orientations that we use, shown in Fig 1. The singly-displaced operators are meant to mock up a diquark-quark coupling, and the doubly-displaced and triply-displaced operators are chosen since they favor the  $\Delta$ -flux and  $Y$ -flux configurations, respectively.

Next, the  $\Phi_{\alpha\beta\gamma,ijk}^{ABC}$  are combined into *elemental* operators  $B_a^F(t)$  having the appropriate flavor structure characterized by isospin, strangeness, *etc.* We work in the  $m_u = m_d$  (equal  $u$  and  $d$  quark masses) approximation, and thus, require that the elemental operators have definite isospin, that is, they satisfy appropriate commutation relations with the isospin operators  $\tau_3, \tau_+, \tau_-$ . Since we plan to compute full correlation matrices, we need not be concerned with forming operators according to an  $SU(3)$  flavor symmetry. Maple code which manipulates Grassmann fields was used to identify maximal sets of linearly independent elemental operators. The operators used are shown in Table 2, and the numbers of such independent operators are listed in this table as well.

The final step in our operator construction is to apply group-theoretical projections to obtain operators which transform irreducibly under all lattice rotation and reflection symmetries:

$$B_a^{\Lambda\lambda F}(t) = \frac{d_\Lambda}{g_{O_h}} \sum_{R \in O_h} \Gamma_{\lambda\lambda}^{(\Lambda)}(R) U_R B_a^F(t) U_R^\dagger, \quad (5)$$

Table 2. Elemental operators for various baryons (left). The numbers of linearly independent elemental operators of each spatial kind (right).

Baryon	Operator	Spatial Type	$\Delta, \Omega$	$N$	$\Sigma, \Xi$	$\Lambda$
$\Delta^{++}$	$\Phi_{\alpha\beta\gamma,ijk}^{uuu}$	single-site	20	20	40	24
$\Sigma^+$	$\Phi_{\alpha\beta\gamma,ijk}^{uus}$	singly-displaced	240	384	624	528
$N^+$	$\Phi_{\alpha\beta\gamma,ijk}^{uud} - \Phi_{\alpha\beta\gamma,ijk}^{duu}$	doubly-displaced-I	192	384	576	576
$\Xi^0$	$\Phi_{\alpha\beta\gamma,ijk}^{ssu}$	doubly-displaced-L	768	1536	2304	2304
$\Lambda^0$	$\Phi_{\alpha\beta\gamma,ijk}^{uds} - \Phi_{\alpha\beta\gamma,ijk}^{dus}$	triply-displaced-T	768	1536	2304	2304
$\Omega^-$	$\Phi_{\alpha\beta\gamma,ijk}^{sss}$	triply-displaced-O	512	1024	1536	1536

where  $\Lambda$  refers to an  $O_h$  irrep,  $\lambda$  is the irrep row,  $g_{O_h}$  is the number of elements in  $O_h$ ,  $d_\Lambda$  is the dimension of the  $\Lambda$  irrep,  $\Gamma_{mn}^{(\Lambda)}(R)$  is a  $\Lambda$  representation matrix corresponding to group element  $R$ , and  $U_R$  is the quantum operator which implements the symmetry operations. The projections in Eq. (5) are carried out using computer software written in the Maple<sup>9</sup> symbolic manipulation language.

#### 4. Field smearing and operator pruning

For single-site (local) hadron operators, it is well known that the use of spatially-smearred quark fields is crucial. For extended baryon operators, one expects quark-field smearing to be equally important, but the relevance and interplay of link-field smearing is less well known. Thus, we decided that a systematic study of both quark-field and link-variable smearing was warranted.

The link variables were smeared  $U \rightarrow \tilde{U}$  using the analytic stout link method of Ref. 10. There are two tunable parameters, the number of iterations  $n_\rho$  and the staple weight  $\rho$ . For the quark-field, we employed gauge-covariant Gaussian smearing

$$\tilde{\Psi}(x) = \left(1 + \frac{\sigma_s^2}{4n_\sigma} \tilde{\Delta}\right)^{n_\sigma} \Psi(x), \quad (6)$$

$$\tilde{\Delta}\Psi(x) = \sum_{k=\pm 1, \pm 2, \pm 3} \left(\tilde{U}_k(x)\Psi(x + \hat{k}) - \Psi(x)\right), \quad (7)$$

where  $\tilde{\Delta}$  denotes the smeared three-dimensional gauge-covariant Laplacian. The two parameters to tune in this smearing procedure are the smearing radius  $\sigma_s$  and the integer number of iterations  $n_\sigma$ .

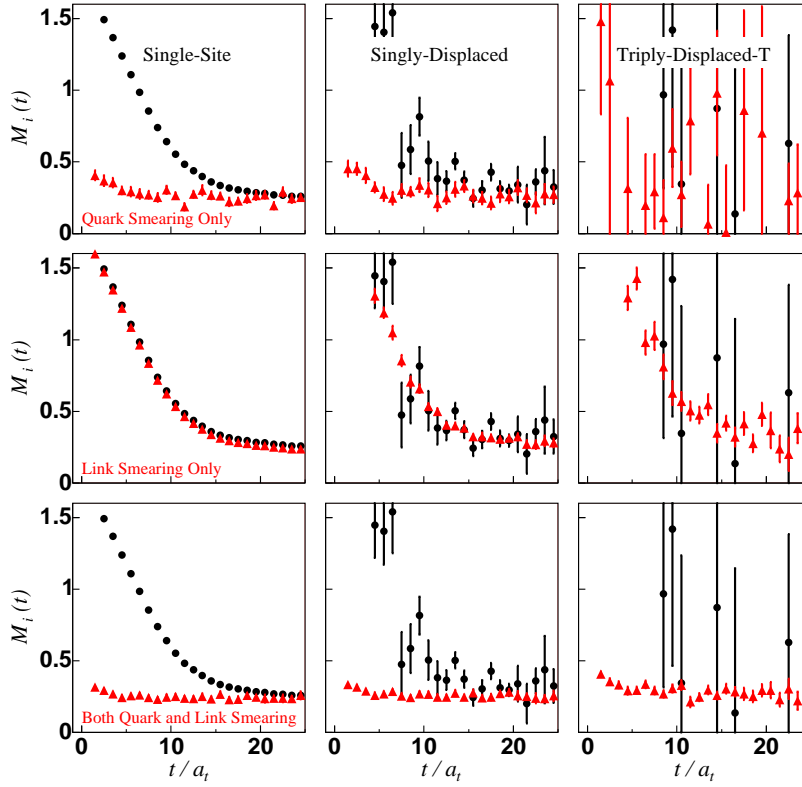


Figure 2. Effective masses  $M(t)$  for unsmeared (circles) and smeared (triangles) operators  $O_{SS}$ ,  $O_{SD}$ ,  $O_{TDT}$ . Top row: only quark-field smearing  $n_\sigma = 32$ ,  $\sigma_s = 4.0$  is used. Middle row: only link-variable smearing  $n_\rho = 16$ ,  $n_\rho\rho = 2.5$  is applied. Bottom row: both quark and link smearing  $n_\sigma = 32$ ,  $\sigma_s = 4.0$ ,  $n_\rho = 16$ ,  $n_\rho\rho = 2.5$  are used, dramatically improving the signal for all three operators. Results are based on 50 quenched configurations on a  $12^3 \times 48$  anisotropic lattice using the Wilson action with  $a_s \sim 0.1$  fm,  $a_s/a_t \sim 3.0$ . The quark mass was chosen so that  $m_\pi \simeq 700$  MeV.

For our tests of the efficacy of quark-field and gauge-link smearing, correlators were computed for three particular nucleon operators: a single-site operator  $O_{SS}$  in the  $G_{1g}$  irreducible representation of the cubic point group, a singly-displaced operator  $O_{SD}$  with a particular choice of each Dirac index, and a triply-displaced-T operator  $O_{TDT}$  with a specific choice of each Dirac index. Our findings are summarized in Fig. 2. The top row shows that applying only quark-field smearing to the three selected nucleon operators significantly reduces couplings to higher-lying states, but the dis-

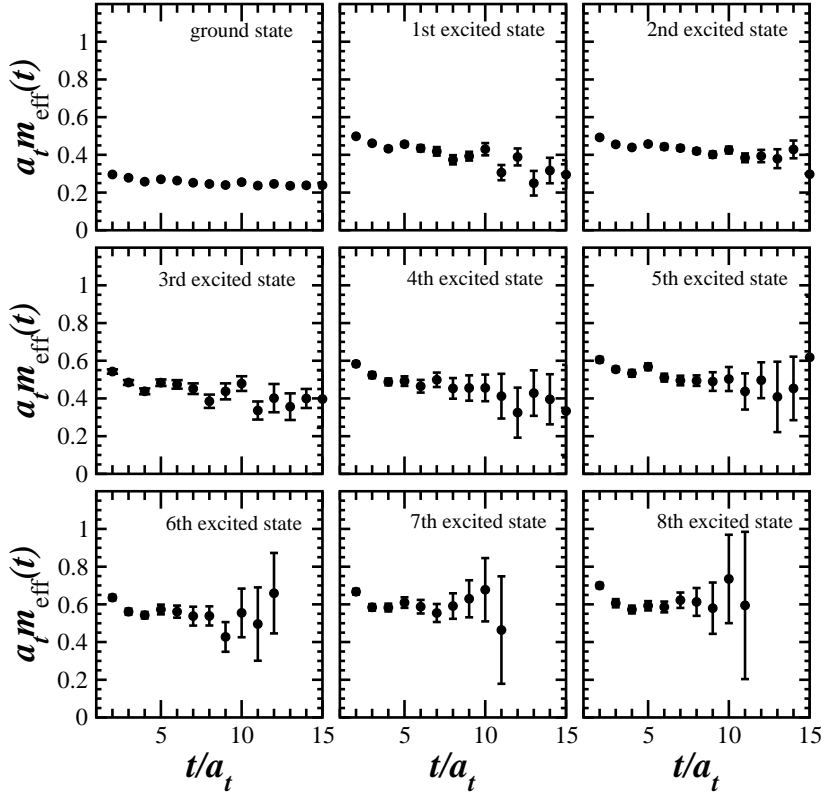


Figure 3. Principal effective masses for the lowest-lying *nine* states in the  $G_{1g}$  nucleon channel. Results are based on 100 quenched configurations on a  $12^3 \times 48$  anisotropic lattice using the Wilson action with  $a_s \sim 0.1$  fm,  $a_s/a_t \sim 3.0$ . The quark mass was chosen so that  $m_\pi \simeq 700$  MeV. Quark-field smearing  $n_\sigma = 32$ ,  $\sigma_s = 3.0$  and link-smearing  $n_\rho = 16$ ,  $n_{\rho\rho} = 2.5$  are used. These principal effective masses come from a  $10 \times 10$  correlation matrix, where 2 singly-displaced, 5 doubly-displaced-I, 2 doubly-displaced-L, and 1 triply-displaced-T operators were chosen.

placed operators remain excessively noisy. The second row illustrates that including only link-field smearing substantially reduces the noise, but does not appreciably alter the effective masses themselves. The bottom row shows dramatic improvement from reduced couplings to excited states and dramatically reduced noise when both quark-field and link-field smearing is applied, especially for the extended operators. The “best” quark-field smearing parameters  $n_\sigma$  and  $\sigma$  were determined by requiring that the effective mass for the three chosen operators reach a plateau as close to the



source as possible. The gauge-link smearing parameters were tuned so as to minimize the noise in the effective masses. One interesting point we also learned was that the preferred link-smearing parameters determined from the static quark-antiquark potential produced the smallest error in the extended baryon operators.

The computation of correlation matrices using hundreds of operators is not feasible, so it is necessary to “prune” out unnecessary operators. The first step in this pruning is to examine the effective masses of the diagonal elements of the correlation matrices to identify and eliminate noisy operators. Keeping only operators with small statistical uncertainties yields a set of about forty to fifty operators in each symmetry channel. We then computed the correlation matrix of this reduced set of operators, examining whether further reductions to the operator sets could be made without increased contamination in the principal effective masses. These computations are still ongoing, but preliminary results are shown in Fig. 3. This figure shows that it is possible to extract at least *nine* levels in a given symmetry channel, a feat which has never before been accomplished. Demonstrating that this number of energy levels can be reliably extracted is an important milestone in our long-term project.

## 5. Conclusion

We have outlined a program to study the resonance spectrum in lattice QCD. The use of the variational method and the need to isolate several energy levels in each channel require a sufficiently broad basis of operators. Having developed suitable group-theory methods to project operators onto the irreducible representations of the cubic group, and having examined the efficacy of both quark- and gauge-link-smearing, we are now identifying a more limited set of operators that we will employ in a large-scale study of the hadron spectrum. Our methods are applicable not only to baryons, but also to mesons, tetra-quark and pentaquark systems, and to states with excited glue. Only by performing such a program can we hope to identify the states of QCD, and in particular their spins and parities, in the continuum limit. Ultimately, when quark loops are included at realistically light quark masses, multi-hadron (baryon-meson) operators must be included in our correlation matrices, and finite-volume techniques will need to be employed to ferret out the baryon resonances from uninteresting scattering states. We are currently exploring different ways of building such operators.

This work was supported by the U.S. National Science Foundation through grants PHY-0354982, PHY-0510020, and PHY-0300065, and by the U.S. Department of Energy under contracts DE-AC05-84ER40150 and DE-FG02-93ER-40762. Computations were performed using the *Chroma* software package<sup>11</sup>.

### References

1. S. Basak, R. Edwards, G. Fleming, U. Heller, C. Morningstar, D. Richards, I. Sato, S. Wallace, *Phys. Rev. D* **72**, 094506 (2005); **72**, 074501 (2005).
2. S. Basak, R. Edwards, G. Fleming, U. Heller, A. Lichtl, C. Morningstar, D. Richards, I. Sato, and S. Wallace, *Proc. Sci. LAT2005*: **076** (2005).
3. C. Michael, *Nucl. Phys. B* **259**, 58 (1985).
4. M. Lüscher and U. Wolff, *Nucl. Phys. B* **339**, 222 (1990).
5. B. DeWitt, *Phys. Rev.* **103**, 1565 (1956).
6. U. Wiese, *Nucl. Phys. B (Proc. Suppl.)* **9**, 609 (1989).
7. M. Lüscher, *Nucl. Phys. B* **364**, 237 (1991).
8. K. Rummukainen and S. Gottlieb, *Nucl. Phys. B* **450**, 397 (1995).
9. Visit the web site <http://www.maplesoft.com>.
10. C. Morningstar and M. Peardon, *Phys. Rev. D* **69**, 054501 (2004).
11. R. Edwards and B. Joo, *Nucl. Phys. B (Proc. Suppl.)* **140**, 832 (2005).